

# Lipase-Catalyzed Copolymerization of $\omega$ -Pentadecalactone with *p*-Dioxanone and Characterization of Copolymer Thermal and Crystalline Properties

Zhaozhong Jiang, Himanshu Azim, and Richard A. Gross\*

NSF I/UCRC for Biocatalysis and Bioprocessing of Macromolecules, Department of Chemical and Biological Sciences, Polytechnic University, Six Metrotech Center, Brooklyn, New York 11201

Maria Letizia Focarete and Mariastella Scandola\*

University of Bologna, Department of Chemistry "G. Ciamician", via Selmi 2, 40126 Bologna, Italy

Received February 3, 2007; Revised Manuscript Received April 11, 2007

*Candida antarctica* Lipase B (CALB), a metal-free enzyme, was successfully employed as catalyst for ring-opening copolymerization of  $\omega$ -pentadecalactone (PDL) with *p*-dioxanone (DO) under mild reaction conditions (<80 °C, atmospheric pressure). Poly(PDL-*co*-DO) with high molecular weight ( $M_w > 30\,000$ ) and a wide range of comonomer contents was synthesized using various PDL/DO feed ratios. During the copolymerization reaction, large ring PDL was found to be more reactive than its smaller counterpart DO, resulting in higher PDL/DO unit ratios in polymer chains than the corresponding PDL/DO monomer ratios in the feed. The copolymers were typically isolated in 50–90 wt % yields as the monomer conversion was limited by the equilibrium between monomers and copolymer.  $^1\text{H}$  and  $^{13}\text{C}$  NMR analysis on poly(PDL-*co*-DO) formed by CALB showed that the copolymers contain nearly random sequences of PDL and DO units with a slight tendency toward alternating arrangements. Copolymerization with PDL was found to remarkably enhance PDO thermal stability. Differential scanning calorimetry (DSC) and wide-angle X-ray scattering (WAXS) results demonstrate high crystallinity in all copolymers over the whole range of compositions. Depending on copolymer composition, the crystal lattice of either PDO or PPDL hosts units of the other comonomer, a behavior typical of an isodimorphic system. In poly(PDL-*co*-DO), both melting temperature and melting enthalpy display a minimum at 70 mol % DO, that is, at the pseudoeutectic composition. WAXS diffractograms show one crystal phase (that of either PPDL or PDO) on either side of the pseudoeutectic and coexistence of PPDL and PDO crystals at the pseudoeutectic.

## Introduction

Poly(*p*-dioxanone) (PDO), poly(glycolide), and poly(lactide) are well-known semicrystalline polymers that are extensively used as bioabsorbable materials for constructing surgical sutures, staples, screws, and reinforcing plates as well as controlled release drug carriers. PDO, a poly(ether-ester), was synthesized originally for coating and textile fiber applications but was found unsuitable because of its high susceptibility to hydrolysis.<sup>1</sup> However, the poly(ether-ester) with fast degradability, desirable physical properties, and excellent biocompatibility was later recognized and was found to serve remarkably well as materials for biomedical applications.<sup>2</sup>

It is well-known that copolymerization is an effective approach to obtain materials with tailored properties that are usually improved with respect to those of the respective homopolymers. In medical applications, the hydrolysis/biodegradation rates and physical properties of PDO-based materials are often controlled and regulated by incorporating other monomers along the polymer backbone. Thus, various *p*-dioxanone-containing copolyesters, including poly(*p*-dioxanone-*co*- $\epsilon$ -caprolactone), poly(*p*-dioxanone-*co*-glycolide), poly(*p*-dioxanone-*co*-lactide), and poly(*p*-dioxanone-*co*-alkylene oxide), have been disclosed and proposed as alternative bioresorbable materials.<sup>3</sup> However, copolymers of *p*-dioxanone (DO) with large ring size lactone monomers, such as  $\omega$ -pentadecalactone (PDL), have not been reported thus far. Poly(PDL-*co*-DO) is of great interest because PDL repeating units have substantially

lower hydrophilicity and hydrolytic susceptibility versus DO units, which should render PDL more effective than smaller ring size lactone monomers (e.g.,  $\epsilon$ -caprolactone, glycolide, lactide) in altering or reducing PDO biodegradation rate. Furthermore, upon hydrolysis and degradation, PDL units would be converted to  $\omega$ -hydroxypentadecanoic acid that represents a typical hydroxyl-substituted fatty acid and that is expected to pose minimal adverse health effects.

Current commercial processes for producing PDO and DO-containing copolyesters employ organometallic catalysts. As indicated in recent patent literature, minimal residual metal contents are essential to ensure safety of these polymeric materials in biomedical applications. Indeed, new synthetic methods are needed to reduce metal concentrations for certain polymer applications.<sup>4</sup> Metal-free enzymatic catalysts would be most desirable for preparing medical grade PDO and related copolyesters. *Candida antarctica* Lipase B (CALB) is a metal-free catalyst and is known to be highly efficient for PDL and other lactone ring-opening polymerizations.<sup>5</sup> CALB-catalyzed processes have recently been reported to synthesize random and block copolymers of 1,5-dioxepan-2-one and  $\epsilon$ -caprolactone<sup>6a,6b</sup> and poly(pentadecalactone-*co*-oxo-crown ether).<sup>6c,6d</sup> Herein, we report for the first time the synthesis of poly(PDL-*co*-DO) copolymers with various PDL/DO unit ratios under mild reaction conditions using metal-free CALB as the catalyst. Copolymer microstructure was analyzed by both proton and carbon-13 NMR spectroscopy. The thermal properties of nearly random poly-

(PDL-*co*-DO) as a function of copolymer composition were investigated by thermogravimetric analysis (TGA) and differential scanning calorimetry (DSC). Wide-angle X-ray scattering (WAXS) analyses were performed to study copolymer crystal structures. In contrast to expected random copolymer behavior, poly(PDL-*co*-DO) samples maintain high crystallinity over the entire compositional range. An explanation for this behavior is presented.

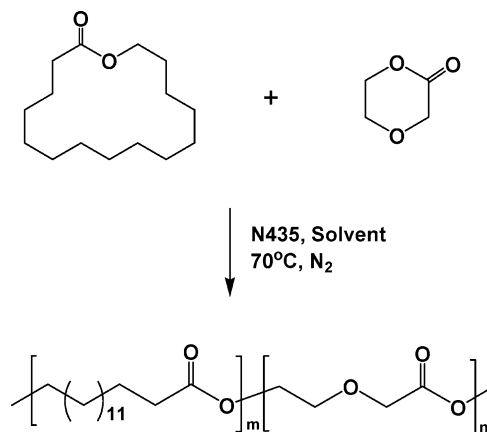
## Experimental Section

**Materials.**  $\omega$ -Pentadecalactone monomer (PDL, 98%), anhydrous toluene, and diphenyl ether were purchased from Aldrich Chemical Co. and were used as received. *p*-Dioxanone (DO), a gift from Johnson and Johnson company, was dried over calcium hydride and then was vacuum distilled under nitrogen. N435 (specific activity 10 000 PLU/g) was a gift from Novozymes (Bagsvaerd, Denmark) and consists of *Candida antarctica* Lipase B (CALB) physically adsorbed within the macroporous resin Lewatit VPOC 1600 (poly[methyl methacrylate-*co*-butyl methacrylate], supplied by Bayer). Lewatit VPOC 1600 has a surface area of 110–150 m<sup>2</sup>/g and an average pore diameter of 100 nm. N435 contains 10 wt % CALB that is located on the outer 100  $\mu$ m of 600  $\mu$ m average diameter Lewatit beads.

**Instrumental Methods.** <sup>1</sup>H and <sup>13</sup>C NMR spectra were recorded on a Bruker AVANCE 300 spectrometer or a Bruker AVANCE 500 spectrometer. The chemical shifts reported were referenced to internal tetramethylsilane (0.00 ppm) or to the solvent resonance at the appropriate frequency. The number-average molecular weights and weight-average molecular weights ( $M_n$  and  $M_w$ , respectively) of polymers were measured by gel permeation chromatography (GPC) using a Waters HPLC system equipped with a model 510 pump, a Waters model 717 autosampler, and a Model 410 refractive index detector with 500, 10<sup>3</sup>, 10<sup>4</sup>, and 10<sup>5</sup> Å Ultrastaygel columns in series. Trisec GPC software version 3 was used for calculations. Chloroform was used as the eluent at a flow rate of 1.0 mL/min. Sample concentrations of 2 mg/mL and injection volumes of 100  $\mu$ L were used. Molecular weights were determined on the basis of a conventional calibration curve generated by narrow polydispersity polystyrene standards from Aldrich Chemical Co. Thermogravimetric analysis (TGA) measurements were performed with a TA Instruments TGA2950 thermogravimetric analyzer from room temperature to 600 °C, at a heating rate of 10 °C/min, in a nitrogen atmosphere. Differential scanning calorimetry (DSC) analysis was carried out using a TA Instruments Q100 DSC equipped with the liquid nitrogen cooling system (LNCS) low-temperature accessory. The temperature scale was calibrated with high-purity standards. DSC scans were performed in the temperature range from –100 °C to 150 °C. Wide-angle X-ray diffraction measurements (WAXS) were carried out at room temperature with a PANalytical X'Pert PRO diffractometer equipped with an XCelerator detector. CuK radiation ( $\lambda = 0.15418$  nm) was used as X-ray source. The degree of crystallinity ( $\chi_c$ ) was evaluated as the ratio of the crystalline peak areas to the total area under the scattering curve.<sup>7</sup> The amorphous and crystalline contributions were calculated by fitting method using the WinFit program.<sup>8</sup> The primary beam and air scattering contribution to the incoherent scattering was considered equal to the contribution of an empty sample holder recorded in the same conditions, which was therefore subtracted from the sample spectrum.

**General Procedures for Preparing Poly(PDL-*co*-DO) Copolymers.** A reaction mixture containing PDL, DO, and N435 (5 wt % vs total monomer, dried under 1.0 mmHg at 50 °C for 18 h) in toluene or diphenyl ether (200 wt % vs total monomer) was magnetically stirred at 70 °C under nitrogen (1 atm) for 26 h. At the end of the reaction, the product mixture was dissolved in chloroform, and the resultant solution was filtered to remove catalyst particles. The filtrate was then concentrated at 50–60 °C under vacuum. A white solid precipitate was obtained by dropwise adding the concentrated polymer solution into magnetically stirred methanol. Precipitated polymer was filtered, was

**Scheme 1.** Ring-Opening Copolymerization between PDL and DO Catalyzed by N435



washed with methanol three times, and was dried overnight at 50 °C in vacuo. The results of <sup>1</sup>H and <sup>13</sup>C NMR spectral analyses were as follows.

Poly(PDL-*co*-DO): (a) <sup>1</sup>H NMR (CDCl<sub>3</sub>) (ppm) PDL units: 4.05–4.13 (m, –CH<sub>2</sub>–CH<sub>2</sub>–(CH<sub>2</sub>)<sub>10</sub>–CH<sub>2</sub>–CH<sub>2</sub>–COO–); 2.32 (2H, m, –CH<sub>2</sub>–CH<sub>2</sub>–(CH<sub>2</sub>)<sub>10</sub>–CH<sub>2</sub>–CH<sub>2</sub>–COO–); 1.62 (4H, br, –CH<sub>2</sub>–CH<sub>2</sub>–(CH<sub>2</sub>)<sub>10</sub>–CH<sub>2</sub>–CH<sub>2</sub>–COO–); 1.26 (20H, br, –CH<sub>2</sub>–CH<sub>2</sub>–(CH<sub>2</sub>)<sub>10</sub>–CH<sub>2</sub>–CH<sub>2</sub>–COO–); DO units: 4.35/4.27 (2H, t, –CH<sub>2</sub>–CH<sub>2</sub>–O–CH<sub>2</sub>–COO–); 4.13–4.19 (m, –CH<sub>2</sub>–CH<sub>2</sub>–O–CH<sub>2</sub>–COO–); 3.80 (2H, br, –CH<sub>2</sub>–CH<sub>2</sub>–O–CH<sub>2</sub>–COO–). (b) Selected <sup>13</sup>C NMR absorptions (CDCl<sub>3</sub>) (ppm): 174.0 (PDL–PDL\*–PDL/DO–PDL\*–PDL, –CH<sub>2</sub>–CH<sub>2</sub>–(CH<sub>2</sub>)<sub>10</sub>–CH<sub>2</sub>–CH<sub>2</sub>–COO–); 173.8 (PDL–PDL\*–DO/DO–PDL\*–DO, –CH<sub>2</sub>–CH<sub>2</sub>–(CH<sub>2</sub>)<sub>10</sub>–CH<sub>2</sub>–CH<sub>2</sub>–COO–); 170.2, 170.13/170.11, 170.0 (PDL–DO\*–PDL, PDL–DO\*–DO/DO–DO\*–PDL, DO–DO\*–DO, –CH<sub>2</sub>–CH<sub>2</sub>–O–CH<sub>2</sub>–COO–); 69.6/69.3 (–CH<sub>2</sub>–CH<sub>2</sub>–O–CH<sub>2</sub>–COO–); 68.5/68.3/68.2 (–CH<sub>2</sub>–CH<sub>2</sub>–O–CH<sub>2</sub>–COO–); 65.1/64.4 (–CH<sub>2</sub>–CH<sub>2</sub>–(CH<sub>2</sub>)<sub>10</sub>–CH<sub>2</sub>–CH<sub>2</sub>–COO–); 63.8/63.2 (–CH<sub>2</sub>–CH<sub>2</sub>–O–CH<sub>2</sub>–COO–); 34.4/34.2 (–CH<sub>2</sub>–CH<sub>2</sub>–(CH<sub>2</sub>)<sub>10</sub>–CH<sub>2</sub>–CH<sub>2</sub>–COO–); resonances at 24.9–29.6 ppm (–CH<sub>2</sub>–CH<sub>2</sub>–(CH<sub>2</sub>)<sub>10</sub>–CH<sub>2</sub>–CH<sub>2</sub>–COO–).

## Results and Discussion

**Ring-Opening Copolymerization of PDL with DO.** Scheme 1 illustrates the general copolymerization reaction between PDL and DO. N435 (5 wt % vs total monomer) catalyzed polymerizations were conducted in dried toluene or diphenyl ether (200 wt % vs total monomer) at 70 °C under nitrogen for 26 h. To synthesize copolymers with different PDL or DO contents, various PDL/DO monomer feed ratios were used. Since excess water in reactions can limit copolymer molecular weights,<sup>9</sup> all reactants and solvents were either obtained predried or were dried prior to polymerization reactions (see Experimental Section).

The choice of solvent for polymerization reactions was determined by the solubility of poly(PDL-*co*-DO) copolymers formed. At  $\leq 80:20$  (mol/mol) DO/PDL monomer feed ratios, toluene is a desirable solvent since it readily dissolved the resultant copolymers. However, at  $>80:20$  DO/PDL monomer feed ratios, the low solubility of copolymers formed in toluene was evident by their precipitation from reaction solutions after approximately 5 h reaction, leading to low polymer molecular weights. Further studies showed that diphenyl ether is a better solvent than toluene for PDL–DO copolymers with high DO contents. Thus, all PDL–DO copolymerization reactions at  $>80:20$  (mol/mol) DO/PDL feed ratio were performed in diphenyl ether to increase copolymer molecular weights. Homopolymers

**Table 1.** N435-Catalyzed Copolymerization of PDL with DO

sample name	PPDL	P80D20	P68D32	P43D57	P29D71	P16D84	PDO
PDL/DO feed ratio (mol/mol)	100:0	70:30	50:50	30:70	20:80	10:90	0:100
solvent	toluene	toluene	toluene	toluene	toluene	Ph <sub>2</sub> O	toluene
isolated yield (wt %) <sup>a</sup>	90%	77%	87%	70%	74%	51%	75%
DO content, mol % <sup>b</sup>	0	20	32	57	71	84	100
DO content, wt %	0	10	17	36	51	69	100
PDL/DO unit ratio	100/0	80/20	68/32	43/57	29/71	16/84	0/100
<i>M<sub>n</sub></i> (kDa)	16200	19800	15500	29100	14800	11300	6200
<i>M<sub>w</sub></i> (kDa)	48600	107000	54300	55900	31200	18900	22900
polydispersity ( <i>M<sub>w</sub></i> / <i>M<sub>n</sub></i> )	3.0	5.4	3.5	1.9	2.1	1.7	3.7

<sup>a</sup> Yield was calculated on the basis of total monomer weight. <sup>b</sup> Calculated from the proton NMR spectra.

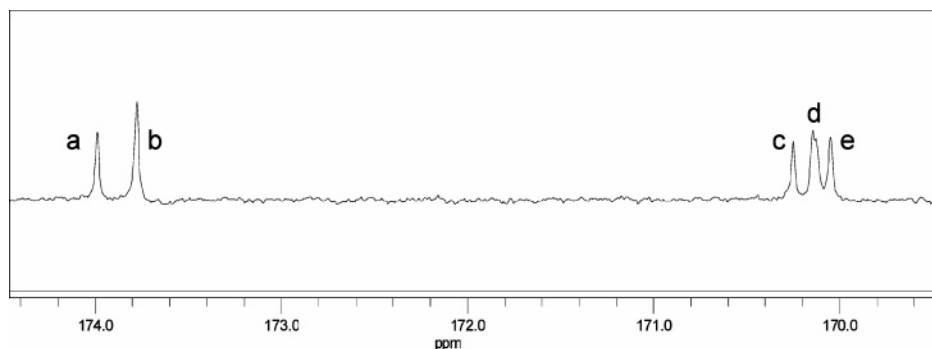


**Figure 1.** Carbonyl C-13 absorptions of P43D57 in CDCl<sub>3</sub>. (a) PDL–PDL\*–PDL and DO–PDL\*–PDL; (b) PDL–PDL\*–DO and DO–PDL\*–DO; (c) PDL–DO\*–PDL; (d) PDL–DO\*–DO and DO–DO\*–PDL; (e) DO–DO\*–DO.

PPDL and PDO were prepared in toluene following procedures analogous to those used for poly(PDL-*co*-DO) synthesis.

The copolymerization results regarding reaction conditions, product yields, polymer molecular weights, and polydispersity are summarized in Table 1. High molecular weight ( $M_w > 30\,000$ ) poly(PDL-*co*-DO) polymers were synthesized by N435-catalyzed polymerization reactions (see Experimental Section). In all cases, PDL content in copolymers exceeded that in the monomer feed, suggesting that N435 favors polymerization of PDL over DO. Isolated yields after polymer precipitation were  $\geq 70\%$  except for the highest DO monomer feed ratio (90 mol %) in which the isolated yield is 51%. Since ring-opening polymerizations involve equilibrium reactions between monomers and copolymer, previous studies have shown that this is an important factor which limits monomer conversions and polymer yield.<sup>10</sup> Given the difficulty in PDL polymerizations by conventional chemical methods,<sup>11</sup> it is expected that similar problems would be encountered if conventional chemical methods were attempted to prepare PDL–DO copolymers. Furthermore, undoubtedly, DO would be more reactive than PDL with conventional chemical catalysts giving copolymers enriched in DO units.

**Structures of Poly(PDL-*co*-DO).** Structures of PDL–DO copolymers with various PDL/DO repeating unit compositions were analyzed by both proton (<sup>1</sup>H) and carbon-13 (<sup>13</sup>C) NMR spectroscopy. Assignment of NMR resonances was made by comparing peak positions for PPDL, PDO homopolymers, and PDL–DO copolymers with different DO content. The ratio of PDL versus DO units in copolymers was calculated from proton NMR absorptions, for example, PDL methylene (–CH<sub>2</sub>–CH<sub>2</sub>–(CH<sub>2</sub>)<sub>10</sub>–CH<sub>2</sub>–CH<sub>2</sub>–COO–) resonances at 2.32 ppm and DO methylene (–CH<sub>2</sub>–CH<sub>2</sub>–O–CH<sub>2</sub>–COO–) resonances at 3.80 ppm, and the results are summarized in Table 1.

Ester carbonyl <sup>13</sup>C NMR resonances of PDL and DO units were observed at approximately 174 and 170 ppm, respectively

**Table 2.** Structures of PDL–DO Copolymers

sample name	P43D57	P29D71	P16D84
Calcd Triads in Random Copolymer <sup>a</sup>			
PDL–PDL*–PDL + DO–PDL*–PDL	0.18	0.08	0.03
PDL–PDL*–DO + DO–PDL*–DO	0.24	0.21	0.13
PDL–DO*–PDL	0.11	0.06	0.02
PDL–DO*–DO + DO–DO*–PDL	0.28	0.29	0.23
DO–DO*–DO	0.19	0.36	0.59
Observed Triads <sup>b</sup>			
PDL–PDL*–PDL + DO–PDL*–PDL	0.16	0.08	0.02
PDL–PDL*–DO + DO–PDL*–DO	0.25	0.22	0.12
PDL–DO*–PDL	0.14	0.07	0.03
PDL–DO*–DO + DO–DO*–PDL	0.28	0.30	0.26
DO–DO*–DO	0.17	0.33	0.57

<sup>a</sup> For a random A–B copolymer, distribution of triad X–Y\*–Z =  $f_x \times f_y \times f_z$  (X, Y, and Z independently equal A or B;  $f_x$ ,  $f_y$ , and  $f_z$  are molar fractions of corresponding repeating units X, Y, and Z in the polymer chains). <sup>b</sup> Calculated from the <sup>13</sup>C NMR spectra.

(Figure 1). The two carbonyl absorptions of PDL units at 173.8 and 174.0 ppm are due to corresponding PDL–PDL\*–DO/DO–PDL\*–DO and PDL–PDL\*–PDL/DO–PDL\*–PDL triads, respectively. The four carbonyl absorptions of DO units at 170.2, 170.13/170.11, and 170.0 are assigned to PDL–DO\*–PDL, PDL–DO\*–DO/DO–DO\*–PDL, and DO–DO\*–DO triads, respectively.

Table 2 shows the distribution of triad structures for copolymers P43D57, P29D71, and P16D84. To quantitatively determine the repeat unit sequence or arrangement of PDL and DO units along copolymer chains, distributions of triad structures for statistically random copolymers at corresponding PDL/DO unit ratios were calculated. The experimental results and theoretically calculated data were compared (Table 2). This analysis shows that PDL–DO copolymers formed by N435

**Table 3.** Thermal Properties and Crystallinity of Poly(PDL-co-DO)

sample	TGA $T_{\max}$ (°C)	WAXS $X_c^a$ (%)	DSC			
			cooling <sup>b</sup> $\Delta H_c$ (J/g)	heating <sup>c</sup>		
				$\Delta H_m$ (PPDL) (J/g)	$\Delta H_c$ (PDO) (J/g)	$\Delta H_m$ (PDO) (J/g)
PPDL	414	63	127	127		
P80D20	412	57	122	123		
P68D32	407	59	105	107		
P43D57	396	56	69	71		
P29D71	389	44	52	49		3
P16D84	334, 389	45	34	21	40	53
PDO	309	58	50		32	82

<sup>a</sup> Crystallinity degree from WAXS ( $\pm 5\%$ ). <sup>b</sup> Cooling run at  $-10$  °C/min. <sup>c</sup> Heating run (20 °C/min) following the cooling run.

catalysis contain nearly random sequences of PDL and DO units with a slight tendency toward alternating sequences. Analysis of the other two copolymers (P80D20, P68D32) showed similar results regarding polymer microstructures.

The copolymerization between PDL and DO could initially form polymer chains with block structures as the result of higher polymerization activity of PDL versus DO. However, by extending the reaction time, PPDL and PDO blocks are converted to random structures through transesterification promoted by CALB catalysis.<sup>12</sup>

**Solid-State Characterization.** Thermal properties of poly(PDL-co-DO) were investigated by TGA and DSC, and the results are summarized in Table 3 together with those of the reference homopolymers. The two homopolymers exhibit different thermal stabilities, where the temperature of maximum degradation rate ( $T_{\max}$ ) of PPDL is about 100 °C higher than that of PDO. All copolymers, with up to 71 mol % of DO units, degrade in a single weight loss step centered at a  $T_{\max}$  that slowly decreases with increasing DO unit content, that is, with increasing amount of the less thermally stable component. Given the large molecular weight difference between the two comonomer units (molecular weight of PDL unit is more than twice that of DO), a relatively small molar amount of PDL (such as 29 mol %) represents a rather large amount by weight (49 wt %), which is sufficient to significantly improve copolymer thermal stability.

A different behavior is shown by the copolymer richest in DO units (84 mol %), which exhibits two degradation steps: (1) one at high temperature close to that of P29D71 copolymer and (2) the other at a lower temperature that corresponds to thermal degradation of DO-rich sequences. The different TGA behavior of P16D84 copolymer can be explained by taking into account the high DO unit content of this sample and the remarkably different thermal stability of the two homopolymers. The TGA data show that copolymerization with PDL is an effective way to enhance PDO thermal stability, provided that PDL content is  $\geq 30$  mol %.

Figure 2 illustrates WAXS diffractograms of all copolymers and homopolymers (PPDL, PDO). The degrees of crystallinity,  $X_c$ , derived from X-ray curves, are listed in Table 3. Both PPDL and PDO are semicrystalline materials with a similar degree of crystallinity and similar X-ray patterns exhibiting main reflections (marked with broken arrows in Figure 2) that appear at close but not identical  $2\theta$  angles. Literature data<sup>13,14</sup> reporting the unit cells of the two polymers are consistent with the observed WAXS patterns. A previous study by the authors<sup>13</sup> showed that PPDL crystallizes with an all-trans chain conformation, in a pseudorthorhombic monoclinic unit cell ( $a = 0.749$  nm,  $b = 0.503$  nm, and  $c$  (fiber axis) = 2.00 nm), whereas PDO was reported to crystallize with a  $2_1$  helix conformation,

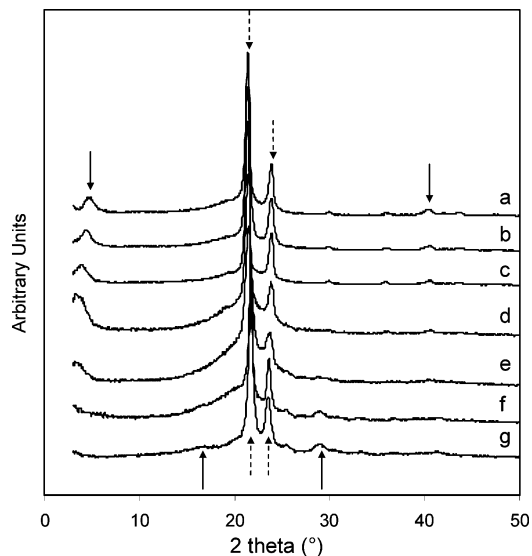


**Figure 2.** WAXS diffractograms of (a) PPDL, (b) P80D20, (c) P68D32, (d) P43D57, (e) P29D71, (f) P16D84, and (g) PDO. Broken and continuous arrows mark main reflections and minor reflections, respectively.

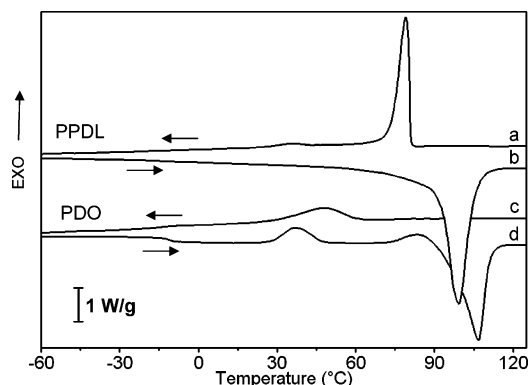


**Figure 3.** DSC curves of PPDL (a, b) and PDO (c, d) homopolymers. Cooling runs were conducted at 10 °C/min (a, c), and subsequent heating runs were at 20 °C/min (b, d).

in an orthorhombic unit cell ( $a = 0.970$  nm,  $b = 0.742$  nm, and  $c$  (chain axis) = 0.682 nm).<sup>14</sup>

Differences in calorimetric behavior for the two homopolymers are appreciable from their corresponding DSC curves displayed in Figure 3. For PPDL, during cooling from the melt (curve a), a crystallization exotherm of remarkable magnitude (see  $\Delta H_c$  in Table 3) appears at low undercooling ( $T_m - T_c = 15$  °C), clearly indicating a strong ability of PPDL chains to

crystallize. In the subsequent heating run, a single melting endotherm is observed at  $T_m = 93$  °C. The absence of a cold crystallization process shows that the polymer completely crystallized during the cooling run. This point is confirmed by that identical crystallization and melting enthalpy values were obtained in cooling and heating runs (Table 3). The melting results of the PPDL used in this work agree with earlier published data on both lipase-catalyzed<sup>15</sup> and chemically synthesized<sup>16</sup> PPDL.

Unlike PPDL, PDO chains are unable to completely crystallize during cooling from the melt at 10 °C/min (note the small exotherm in curve 3c). Indeed, in the subsequent heating curve, the polymer shows cold crystallization over a broad temperature range prior to melting ( $T_m = 107$  °C). The endotherm represents fusion of both crystals formed during cooling and those formed or recrystallized during the heating run, as demonstrated by the melting enthalpy that is identical to the sum of the enthalpies of the two crystallization phenomena. To our knowledge, this is the first report on calorimetric properties of an enzymatically synthesized PDO sample. The DSC results obtained are in agreement with previous literature data on chemically synthesized PDO.<sup>2f,17</sup>

Another difference in the calorimetric behavior of PPDL and PDO homopolymers regards their glass transitions. As previously reported,<sup>15</sup> PPDL crystallizes so quickly from the melt that it cannot be quenched effectively enough to give a sample with a large amorphous fraction, whereas this is readily achievable with PDO. As a consequence, the glass-transition temperature ( $T_g$ ) of PPDL is not easily obtained by DSC but is better revealed by relaxation techniques (a value of  $T_g = -27$  °C was earlier obtained by dynamic mechanical analysis<sup>15</sup>). In contrast, the PDO homopolymer after melt quenching exhibits an intense glass transition in the DSC curve at  $T_g = -10$  °C, in agreement with literature results.<sup>2f,17</sup> In summary, the two reference homopolymers investigated in the present work show a remarkably different crystallization behavior that alters the ability to observe corresponding  $T_g$  transitions by DSC.

Poly(PDL-co-DO) of varying composition was subjected to the same thermal cycle described above for the two homopolymers. Figure 4 compares DSC curves of all copolymers together with those of homopolymers with separate cooling and heating runs. Upon first inspection, DSC patterns appear to change gradually with copolymer composition, both in cooling and subsequent heating scans. Remarkably, all copolymers, independent of composition, show crystallization and melting phenomena.

As discussed above, the poly(PDL-co-DO) copolymers are nearly random polymers. According to common knowledge,<sup>18</sup> random copolymers are expected to show a progressive decrease in crystallinity with increasing comonomer content and degree of randomness, unless the repeat units undergo isomorphous substitution. In the present case, given the fact that the homopolymers of the two repeat units (PDL and DO) have different crystal structures, isomorphism of repeat units should not be expected. Therefore, increasing amounts of DO units within PDL sequence upon copolymerization should lead to a substantial decrease in crystallinity relative to PPDL.

In contrast to expected random copolymer behavior, poly(PDL-co-DO) samples maintain high crystallinity over the entire compositional range. This result was obtained from WAXS diffractograms reported in Figure 2. Degree of crystallinity values are collected in Table 3. Even an equimolar nearly random copolymer, such as P43D57, develops an amount of crystallinity close to 60%.

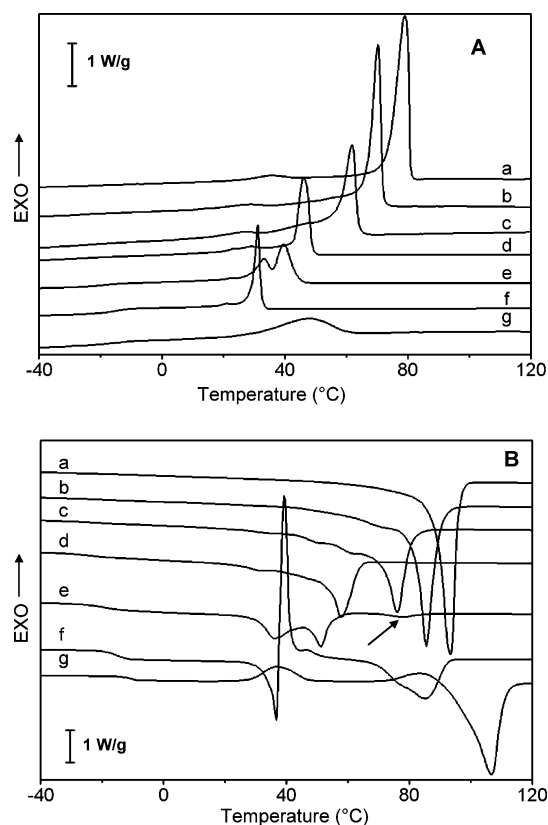


**Figure 4.** DSC curves of poly(PDL-co-DO) and respective homopolymers. (A) Cooling runs at 10 °C/min. (B) Heating runs at 20 °C/min for (a) PPDL, (b) P80D20, (c) P68D32, (d) P43D57, (e) P29D71, (f) P16D84, and (g) PDO.

To gain further understanding on this unusual behavior, DSC curves of copolymers (Figure 4) were analyzed with the aid of corresponding WAXS diffractograms (Figure 2). In Figure 2, all copolymers up to P43D57 show X-ray diffractograms very similar to that of PPDL, with main reflections located at the same positions as those of the homopolymer (see broken and solid arrows). Analysis of DSC cooling scans in Figure 4A shows that a single, remarkably sharp exotherm appears in all copolymers up to 57 mol % DO, at a temperature that decreases with increasing DO content. The corresponding subsequent heating runs reported in Figure 4B show a rather sharp melting endotherm whose  $T_m$  decreases with increasing DO content. The PPDL exotherm in the cooling run (Figure 4A) starts abruptly and develops a typical sharp shape, different from that (very broad) of the PDO homopolymer. Comparative analysis of Figures 2 and 4 suggests that the crystallinity developed in copolymers, at least up to 57 mol % DO units, is associated with a PPDL-type crystal phase. This implies that, up to P43D57, DO units can crystallize in the PPDL crystal lattice, thus justifying the high crystalline content of all copolymers with DO  $\leq$  57 mol %.

Poly(PDL-co-DO) samples with higher DO content (i.e., P29D71 and P16D84) exhibit more complex thermal and crystallographic behavior than the other copolymers. One difficulty in analyzing the diffractograms of poly(PDL-co-DO) in Figure 2 is related to the apparent similarity of the  $2\theta$  region between 20° and 25° in the WAXS patterns of the reference homopolymers. However, besides the two main reflections located in the central spectral region (broken arrows), minor reflections (solid arrows) at  $2\theta = 2-5^\circ$  for PPDL and at  $2\theta = 29^\circ$  for PDO are unique to the respective homopolymers and, therefore, are useful in identifying the crystal phase of copoly-

mers. Analysis of WAXS diffractograms for the two copolymers rich in DO units indicates that PDO reflections, and hence the crystal phase of PDO, are present in both samples (Figure 2). In P29D71, the PDO phase seems to coexist with PPDL-type crystals, whereas in sample P16D84, only PDO reflections are appreciable in the WAXS diffractogram.

Evidence collected so far indicates that poly(PDL-*co*-DO) exhibits crystallinity over the entire composition range but with two crystal phases that are stable in different copolymer composition regions. DSC curves of the two copolymers rich in DO units (71 mol % and 84 mol %), reported in Figure 4, are difficult to interpret compared with those of the other samples. The 71 mol % DO copolymer shows a double-peak crystallization exotherm (Figure 4A), and in a subsequent heating run it melts over two distinct temperature ranges (Figure 4B). The first melting endotherm has multiple peaks (36 °C and 51 °C), whereas the second very small fusion (see arrow in Figure 4B) is located at a higher temperature ( $T_m = 78$  °C). The low-temperature multiple endotherm is tentatively associated with melting and recrystallization of PPDL-type crystals, because its temperature location follows the decreasing trend of the previous samples richer in PDL units. Moreover, the additional high-temperature fusion process of P29D71 is attributed to melting of a very small amount of PDO-type crystals. These assignments are consistent with WAXS results discussed above, which showed the presence of both PPDL and PDO crystal patterns in the diffractogram of P29D71.

A hypothesis to explain the observed calorimetric behavior of this sample is the following: during the cooling run, crystallization of PPDL-type crystals starts in the temperature range typical of PDO crystallization (compare curves e and g in Figure 4A). Hence, as the PPDL crystals form, they act as heterogeneous nucleants for PDO-type crystals. However, the latter cannot grow much owing to continued cooling that inhibits this process while promoting fast crystallization of a PPDL-type phase. Hence, the PDO phase formed in P29D71 during cooling is modest.

Regarding the P16D84 copolymer, the DSC curve in Figure 4A shows one crystallization exotherm that is attributed to crystallization of the PPDL-phase, consistent with the sharp shape of the exotherm (see above). Though the DO content is higher in this copolymer than in P29D71, no efficient heterogeneous nucleation is provided by the PPDL crystals for PDO crystallization in P16D84, owing to the low-temperature range where PPDL crystals appear during cooling (Figure 4A). The subsequent heating run of P16D84 (Figure 4B) is quite complex. Several phenomena can be observed: a rather sharp low-temperature melting, incomplete owing to overlapping with a strong exothermal phenomenon, and a final high-temperature fusion. This behavior was confirmed by analyzing different sample portions and obtaining perfectly reproducible DSC scans. To gain further understanding on this peculiar thermal behavior, the crystallization and melting enthalpies reported in Table 3 for this copolymer have been analyzed in detail.

The melting endotherm at high temperature ( $T_m = 85$  °C) is reasonably attributed to the melting of PDO-type crystals, given the high DO content in this copolymer and the  $T_m$  value close to that of the PDO homopolymer. This endotherm is characterized by a value of  $\Delta H_m = 53$  J/g and is preceded by a cold crystallization exotherm with  $\Delta H_c = 40$  J/g (Table 3) that is clearly underestimated owing to overlapping with the sharp low-temperature melting process (peak temperature = 37 °C,  $\Delta H_m = 21$  J/g). This latter endothermal phenomenon is attributed to melting of PPDL-type crystals formed during the cooling run

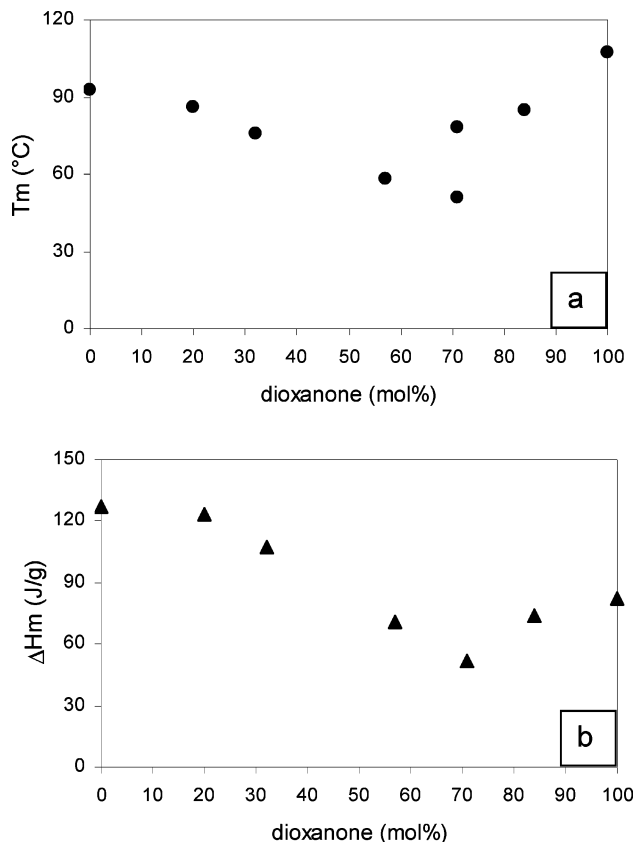


**Figure 5.** (a) Melting temperature (heating run at 20 °C/min after controlled cooling at 10 °C/min) and (b) total melting enthalpy of poly(PDL-*co*-DO) as a function of molar composition.

(sharp exotherm in Figure 4A). It is therefore reasonable to attribute the difference ( $53$  J/g ( $\Delta H_m$ ) –  $40$  J/g ( $\Delta H_c$ ) =  $13$  J/g ( $\Delta H_c$ )) to the missing crystallization enthalpy of the PDO phase, compensated in the exo–endo phenomena appearing in the heating scan. This enthalpy value must be added not only to the cold crystallization of the PDO phase, thus matching crystallization and melting enthalpies, but also to the low-temperature fusion of the PPDL phase. As a result, a value of  $\Delta H_m = 21$  J/g +  $13$  J/g =  $34$  J/g is obtained, which agrees perfectly with the crystallization enthalpy of the PPDL phase in the cooling run ( $\Delta H_c = 34$  J/g).

In summary, the DSC curve of P16D84 (Figure 4B) shows that, after melting of the PPDL crystal phase, a PDO-type phase develops upon heating, which is likely to incorporate PDL units. The above discussion regarding this complex system is finalized through the analysis of the melting temperatures of all copolymers. The data obtained after controlled cooling at 10 °C/min are reported in Figure 5a. Only one  $T_m$  is observed up to a composition of 57 mol % of DO, which is attributed to fusion of a PPDL-type crystal phase. Also, only one  $T_m$  is plotted for P16D84, which is associated with melting of PDO-type crystals (no temperature is reasonably attributable to the incomplete sharp endotherm at 37 °C). For the copolymer containing 71 mol % of DO, two melting temperatures are reported: (1) a low  $T_m$  (temperature of the high melting peak in the multiple endotherm) associated with melting of PPDL-type crystals and (2) a high  $T_m$  corresponding to the small melting endotherm of PDO-type crystals. The total melting enthalpy for each copolymer is also plotted as a function of composition in Figure 5b and shows a minimum in correspondence to copolymer P29D71.

The experimental evidence collected in the course of this investigation suggests that, depending on copolymer composi-

tion, both PDO and PDDL crystal lattices can host units of the other comonomer. For the copolymer composition around 70 mol % DO, the crystal phase changes from one lattice to the other with both crystal types found side by side. The described behavior was identified as isodimorphism by Natta et al.<sup>19</sup> and Allegra and Bassi,<sup>20</sup> and the composition where the  $T_m$  versus concentration content shows a minimum is denoted as pseudoeutectic.<sup>18a,19b</sup> For poly(PDL-*co*-DO), the minimum of  $T_m$  occurs around 70 mol % DO where two crystal phases coexist. An earlier paper by the authors<sup>21</sup> showed the isodimorphic behavior of random poly(3-hydroxybutyrate-*co*-3-hydroxyvalerate) PHBV copolymers. Like the presently investigated poly(PDL-*co*-DO), PHBV showed a minimum in both  $T_m$  and  $\Delta H_m$  at intermediate copolymer composition. The decrease of both parameters toward a minimum reflects the difficulty of either crystal lattice to accommodate increasing amounts of guest monomer units during cocrystallization.

Previously investigated PDL-based copolymer systems<sup>22</sup> showed isomorphism. In such systems, both comonomer units crystallized in the same crystal lattice, whose parameters continuously changed from those of one homopolymer to those of the other. In contrast, PDL-DO copolymers show isodimorphic behavior. Owing to the remarkable difference in crystallization kinetics of the two homopolymers, the amount and type of crystal phase that develops upon solidification from the melt is highly dependent on the sample's thermal history. A deeper investigation on the role played by crystallization kinetics on this copolymer system is in progress, and further evidence for isodimorphic behavior of poly(PDL-*co*-DO) will be reported in a separate paper.

### Conclusions

This work represents the first report where high molecular weight copolyesters containing DO units were synthesized using a metal-free enzyme catalyst. The synthesis of poly(PDL-*co*-DO) was performed so that copolymers possess nearly random sequences of comonomer units along chains. Copolymerization with PDL was found to be an effective way to enhance PDO thermal stability provided that the PDL content is  $\geq 30$  mol %. All copolymers were highly crystalline, even that with almost equimolar comonomer content (P43D57), and had close-to-random unit distribution. Depending on copolymer composition, both PDO and PDDL crystal lattices were able to host units of the other comonomer. This behavior was interpreted as isodimorphism of poly(PDL-*co*-DO). The two homopolymers differ in hydrophilicity, the DO unit being much more hydrophilic than the long PDL unit. A practical implication of this intrinsic difference is that hydrophilicity of PDL-DO copolymers, and hence their rate of hydrolytic degradation, can be modulated by systematic changes in copolymer composition. Compositional changes also influence overall sample crystallinity, thereby providing an additional parameter that can be tuned to control hydrolytic degradation rate. Copolymerization of PDL and DO is expected to produce materials with good mechanical properties and tailored hydrophilicity for targeted biomedical applications.

**Acknowledgment.** We thank the National Science Foundation Industrial/University Cooperative Research Center for Biocatalysis and Bioprocessing of Macromolecules at the Polytechnic University and the Italian Ministry for University and Research (MUR) for their financial support of this work.

### References and Notes

- (1) (a) Schultz, H. S. U.S. Patent 3,063,967, 1962. (b) Schultz, H. S. U.S. Patent 3,063,968, 1962.
- (2) (a) Doddi, N.; Versfelt, C. C.; Wasserman, D. U.S. Patent 4,052,988, 1977. (b) Ray, J. A.; Doddi, N.; Regula, D.; Williams, J. A.; Melveger, A. *Surg., Gynecol. Obstet.* **1981**, *153* (4), 497–507. (c) Yang, K.-K.; Wang, X.-L.; Wang, Y.-Z.; Huang, H.-X. *Mater. Chem. Phys.* **2004**, *87* (1), 218–221. (d) Sabino, M. A.; Albuérne, J.; Mueller, A. J.; Brisson, J.; Prud'homme, R. E. *Biomacromolecules* **2004**, *5* (2), 358–370. (e) Pezzin, A. P. T.; Duek, E. A. R. *Polym. Degrad. Stab.* **2002**, *78* (3), 405–411. (f) Yang, K.-K.; Wang, X.-L.; Wang, Y.-Z. *J. Macromol. Sci., Part C: Polym. Rev.* **2002**, *C42*, 373–398.
- (3) (a) Bezwada, R. S.; Cooper, K.; Erneta, M. U.S. Patent 5,951,997, 1999. (b) Bezwada, R. S.; Cooper, K.; Jamiolkowski, D. D.; Newman, H. D., Jr. U.S. Patent 5,633,343, 1997. (c) Bezwada, R. S.; Cooper, K. U.S. Patent 5,868,788, 1999. (d) Bezwada, R. S.; Cooper, K. L. U.S. Patent 6,113,624, 2000. (e) Shikunami, Y.; Kawarada, H.; Nishi, C. U.S. Patent 6,387,391, 2000. (f) Bezwada, R. S.; Shalaby, S. W. U.S. Patent 5,019,094, 1991. (g) Seo, M. H.; Choi, I. J. U.S. Patent 6,599,519, 2003. (h) Hong, J. T.; Cho, N. S.; Yoon, H. S.; Kim, T. H.; Lee, D. H.; Kim, W. G. *J. Polym. Sci., Part A: Polym. Chem.* **2005**, *43* (13), 2790–2799. (i) Andjelic, S.; Jamiolkowski, D. D.; Kelly, B. M.; Newman, H. *Macromolecules* **2003**, *36* (21), 8024–8032. (j) Bhattarai, N.; Kim, H. Y.; Cha, D. I.; Lee, D. R.; Yoo, D. I. *Eur. Polym. J.* **2003**, *39* (7), 1365–1375.
- (4) Akieda, H.; Shioya, Y.; Kajita, M.; Ozu, K. U.S. Patent 6,448,367, 2002.
- (5) (a) Bisht, K. S.; Henderson, L. A.; Gross, R. A.; Kaplan, D. L.; Swift, G. *Macromolecules* **1997**, *30*, 2705–2711. (b) Gross, R. A.; Kumar, A.; Kalra, B. *Chem. Rev.* **2001**, *101* (7), 2097–2124.
- (6) (a) Srivastava, R. K.; Albertsson, A. C. *Biomacromolecules* **2006**, *7*, 2531–2538. (b) Srivastava, R. K.; Albertsson, A. C. *Macromolecules* **2006**, *39*, 46–54. (c) van der Mee, L.; Antens, J.; van de Kruijs, B.; Palmans, A. R. A.; Meijer, E. W. *J. Polym. Sci., Part A: Polym. Chem.* **2006**, *44*, 2166. (d) Magusin, P. C. M. M.; Mezari, B.; van der Mee, L.; Palmans, A. R. A.; Meijer, E. W. *Macromol. Symp.* **2005**, *230*, 126.
- (7) Kakudo, M.; Kasai, N. *X-Ray Diffraction by Polymers*; American Elsevier Publishing: New York, 1972; Chapters 12 and 13.
- (8) Krumm, S. *Acta Univ. Carol. Geol.* **1994**, *38*, 253.
- (9) Mei, Y.; Kumar, A.; Gross, R. A. *Macromolecules* **2002**, *35*, 5444–5448.
- (10) (a) Nishida, H.; Yamashita, M.; Endo, T.; Tokiwa, Y. *Macromolecules* **2000**, *33* (19), 6982–6986. (b) Esteves, L. M.; Marquez, L.; Mueller, A. J. *J. Appl. Polym. Sci.* **2005**, *97* (2), 659–665.
- (11) Nomura, R.; Ueno, A.; Endo, T. *Macromolecules* **1994**, *27*, 620–621.
- (12) (a) Kumar, A.; Gross, R. A. *J. Am. Chem. Soc.* **2000**, *122*, 11767–11770. (b) Kumar, A.; Kalra, B.; Dekhterman, A.; Gross, R. A. *Macromolecules* **2000**, *33*, 6303–6309.
- (13) Gazzano, M.; Malta, V.; Focarete, M. L.; Scandola, M.; Gross, R. A. *J. Polym. Sci., Part B: Polym. Phys.* **2003**, *41*, 1009–1013.
- (14) Furuhashi, Y.; Nakayama, A.; Monno, T.; Kawahara, Y.; Yamane, H.; Kimura, Y.; Iwata, T. *Macromol. Rapid Commun.* **2004**, *25*, 1943–1947.
- (15) Focarete, M. L.; Scandola, M.; Kumar, A.; Gross, R. A. *J. Polym. Sci., Part B: Polym. Phys.* **2001**, *39*, 1721–1729.
- (16) (a) Lebedev, B.; Yevstropov, A. *Makromol. Chem.* **1984**, *185*, 1235–1253. (b) Skoglund, P.; Fransson, Å. *Polymer* **1998**, *39*, 1899–1906. (c) Skoglund, P.; Fransson, Å. *Polymer* **1998**, *39*, 3143–3146. (d) Zhong, Z.; Dijkstra, P. J.; Feijen, J. *Macromol. Chem. Phys.* **2000**, *201*, 1329–1333. (e) Jedlinski, Z.; Juzwa, M.; Adamus, G.; Kowalczyk, M. *Macromol. Chem. Phys.* **1996**, *197*, 2923–2929.
- (17) (a) Ishikiriya, K.; Pyda, M.; Zhang, G.; Forschner, T.; Grebowicz, J.; Wunderlich, B. *J. Macromol. Sci.: Phys.* **1998**, *B37*, 27–44. (b) Sabino, M. A.; Feijoo, J. L.; Müller, A. J. *Macromol. Chem. Phys.* **2000**, *201*, 2687–2698. (c) Sabino, M. A.; Ronca, G.; Müller, A. J. *J. Mater. Sci.* **2000**, *35*, 5071–5084. (d) Pezzin, A. P. T.; Alberda van Ekenstein, G. O. R.; Duek, E. A. R. *Polymer* **2001**, *42*, 8303–8306.
- (18) (a) Wunderlich, B. *Macromolecular Physics*; Academic Press: New York, 1980; Vol. 1, Chapter II. (b) Mark, J. E.; Eisenberg, A.; Graessley, W. W.; Mandelkern, L.; Koenig, J. L. *Physical Properties of Polymers*; American Chemical Society: Washington, DC, 1984; Chapter 4.

- (19) (a) Natta, G.; Corradini, P.; Sianesi, D.; Morero, D. *J. Polym. Sci.* **1961**, *51*, 527–539. (b) Natta, G.; Allegra, G.; Bassi, I. W.; Sianesi, D.; Caporiccio, G.; Torti, E. *J. Polym. Sci., Part A* **1965**, *3*, 4263–4278.
- (20) Allegra, G.; Bassi, I. W. *Adv. Polym. Sci.* **1969**, *6*, 549–574.
- (21) Scandola, M.; Ceccorulli, G.; Pizzoli, M.; Gazzano, M. *Macromolecules* **1992**, *25*, 1405–1410.
- (22) (a) Focarete, M. L.; Gazzano, M.; Scandola, M.; Gross, R. A. *Macromolecules* **2002**, *35*, 8066–8071. (b) Kalra, B.; Kumar, A.; Gross, R. A.; Baiardo, M.; Scandola, M. *Macromolecules* **2004**, *37*, 1243–1250. (c) Ceccorulli, G.; Scandola, M.; Kumar, A.; Kalra, B.; Gross, R. A. *Biomacromolecules* **2005**, *6*, 902–907.

BM070138A